THE UNIVERSITY OF RHODE ISLAND

University of Rhode Island
DigitalCommons@URI

Physics Faculty Publications

Physics

2015

Enhancement of Radiation Effect on Cancer Cells by Gold-pHLIP

Michael P. Antosh

Dayanjali D. Wijesinghe
University of Rhode Island

See next page for additional authors

Follow this and additional works at: https://digitalcommons.uri.edu/phys_facpubs

Authors

Michael P. Antosh, Dayanjali D. Wijesinghe, Samana Shrestha, Robert Lanou, Yun Hu Huang, Thomas Hasselbacher, David Fox, Nicola Neretti, Shouheng Sun, Natallia Katenka, Leon N. Cooper, Oleg A. Andreev, and Yana K. Reshetnyak

Enhancement of radiation effect on cancer cells by gold-pHLIP

Michael P. Antosh[a,b], Dayanjali D. Wijesinghe[c], Samana Shrestha[c], Robert Lanou[b], Yun Hu Huang[b], Thomas Hasselbacher[a], David Fox[a], Nicola Neretti[a,d], Shouheng Sun[e], Natallia Katenka[f], Leon N Cooper[a,b,1], Oleg A. Andreev[c], and Yana K. Reshetnyak[c,1]

[a]Institute for Brain and Neural Systems and [b]Department of Physics, Brown University, Providence, RI 02912; [c]Physics Department, University of Rhode Island, Kingston, RI 02881; [d]Department of Molecular Biology, Cell Biology and Biochemistry and [e]Department of Chemistry, Brown University, Providence, RI 02912; and [f]Department of Computer Science and Statistics, University of Rhode Island, Kingston, RI 02881

Previous research has shown that gold nanoparticles can increase the effectiveness of radiation on cancer cells. Improved radiation effectiveness would allow lower radiation doses given to patients, reducing adverse effects; alternatively, it would provide more cancer killing at current radiation doses. Damage from radiation and gold nanoparticles depends in part on the Auger effect, which is very localized; thus, it is important to place the gold nanoparticles on or in the cancer cells. In this work, we use the pH-sensitive, tumor-targeting agent, pH Low-Insertion Peptide (pHLIP), to tether 1.4-nm gold nanoparticles to cancer cells. We find that the conjugation of pHLIP to gold nanoparticles increases gold uptake in cells compared with gold nanoparticles without pHLIP, with the nanoparticles distributed mostly on the cellular membranes. We further find that gold nanoparticles conjugated to pHLIP produce a statistically significant decrease in cell survival with radiation compared with cells without gold nanoparticles and cells with gold alone. In the context of our previous findings demonstrating efficient pHLIP-mediated delivery of gold nanoparticles to tumors, the obtained results serve as a foundation for further preclinical evaluation of dose enhancement.

tumor | acidity | targeting | gold nanoparticles | radiation

Gold is an inert and generally nontoxic material with unique properties suitable for many applications such as cancer diagnosis and treatment (1–7). Nanometer-size gold particles have recently been shown to increase radiation damage to tumors (2, 8–11). With enhanced radiation, the same level of tumor killing can be had with less radiation exposure for a patient, reducing the adverse effects of radiation treatments. Similarly, more tumor killing can be had while using the same levels of radiation that are currently given.

The increase in radiation effectiveness with gold nanoparticles is largely a result of two causes. First, gold is capable of absorbing radiation at a significantly higher rate than tissue: up to about 100 times more for keV energies (2). Second, gold nanoparticles that interact with radiation can release extra electrons via the Auger effect. The Auger effect occurs when an atom releases electrons postionization. Multiple electrons, called Auger electrons, can be released per ionization. The Auger electrons usually have low enough energy that their effect is localized to the area surrounding the gold nanoparticles; see, for example, figure 1 in ref. 11. Thus, it is very important to effectively deliver gold nanoparticles to cancer cells in tumors and to locate them near DNA or other vital cellular structures and components.

Specific delivery can be accomplished by conjugating gold (or other nanoparticles) to antibodies or ligands that target overexpressed proteins on cancer cell surfaces; this approach has been actively explored for many years for the delivery of small molecules. However, several recent studies have raised serious questions about the efficacy of targeting ligands on nanoparticle accumulation in tumor tissues. Multiple reports have shown that targeted nanoparticles did not lead to increased tumor

accumulation over nontargeted controls, although increased cellular uptake was observed in each case (12–14). In addition, histologic studies showed that antibodies conjugated with gold nanoparticles do not penetrate deeply into tumors, but mostly stain peripheral tumor regions (15). The direct injection of micrometer-sized gold particles does not lead to tumor targeting, as particles stayed only at the injection site and were not able to diffuse even within a tumor, hindering tumor coverage (16).

Our approach is based on the targeting of tumor acidity, which correlates with tumor malignancy (17–19). The pH-sensitive targeting agents we are developing are based on the action of a family of pHLIPs (pH Low-Insertion Peptides), which can "sense" acidity at the surface of cancer cells and deliver diagnostic and therapeutic molecules to tumors of different origins (20–25). It was shown that pHLIP can promote fusion of liposomes with cancer cells and cellular delivery of various payloads (26, 27), including small gold nanoparticles (26). Recently, pHLIP was successfully used for the targeting of various nanoparticles to tumors and other acidic diseased tissue (28–31).

pHLIP has also been used to mediate pH-controlled delivery of both 13-nm water-soluble gold nanoparticles coated with luminescent europium into human platelets in vitro (32) and 1.4-nm gold nanoparticles to tumors (33). Intratumoral and i.v. administrations of both demonstrated a significant enhancement of tumor uptake of 1.4-nm gold nanoparticles conjugated with

Significance

Nanometer-sized gold particles are shown to increase the effectiveness of radiation in killing cancer cells. Improved radiation effectiveness allows less radiation to be used, reducing adverse effects to patients. Alternatively, more cancer killing could be possible while using current radiation doses. Here we used pH Low-Insertion Peptide (pHLIP) to tether gold nanoparticles to membranes of cancer cells. This increases their effectiveness because the radiation/particle effect is very localized. We find that pHLIP significantly increases the amount of gold particles in cancer cells, as well as the amount of cancer cell death from radiation. This methodology is promising for clinical research, as previous results show efficient targeting of gold nanoparticles to tumors by pHLIP.

pHLIP. Statistically significant reduction of gold accumulation was observed in acidic tumors and kidney when pH-nonsensitive K-pHLIP was used as a vehicle, suggesting an important role of pH in the pHLIP-mediated targeting of gold nanoparticles.

In this work, we made another important step toward clinical application of 1.4-nm gold nanoparticles conjugated with pHLIP. We show that pHLIP can deliver gold to cellular components in a pH-dependent manner and can enhance radiation damage in cells.

Results

In this work we used 1.4-nm-diameter gold clusters functionalized with maleimide. Maleimide-gold clusters were conjugated with WT-pHLIP containing a single Cys residue at the N terminus:

ACEQNPIYWARYADWLFTTPLLLLDLALLVDADET

After conjugation, the construct was purified, lyophilized, redissolved in DMSO, quantified, and used in experiments with cells. As a control (gold alone), we used nonfunctionalized 1.4-nm gold clusters.

Cellular Uptake and Distribution of Gold. We investigated uptake of gold nanoparticles at normal and low pHs (pH 7.4 and 6.0, respectively), with and without pHLIP on human lung carcinoma (A549 cells). At pH 6.0, pHLIP was found to increase cellular uptake of gold nanoparticles by 34% compared with gold nanoparticles alone (P value = 0.023) (Fig. 1 and SI Appendix, Table S1). The uptake of gold-pHLIP at pH 6.0 increased by 53% compared with the uptake at pH 7.4 (P value = 0.008). The uptake of gold alone was also enhanced at pH 6.0 compared with pH 7.4 (P value = 0.014). The uptake of gold-pHLIP was ~60% of the treated dose (1.8 μg), which was about 1.1 μg gold. Because each treatment had ~1 million cells, the amount of gold per cell was ~1.1×10^{-6} μg.

Light microscopy was used to establish the distribution of gold nanoparticles in cells. Bright field images of cells treated with gold-pHLIP or gold alone and enhanced with silver are shown in Fig. 2. The cellular uptake of gold-pHLIP is higher compared with the uptake of gold alone (Fig. 2 A and B; the images are taken using a 20× objective). The representative bright field image of a cell treated with gold-pHLIP and enhanced with silver obtained at high magnification is shown in Fig. 2C (the image is taken using a 100× objective). The overlay of fluorescent images of nuclear stained with DAPI (blue) and cellular membrane stained with HQ Silver deposited on the gold-nanoparticles (red) are shown in Fig. 2D. The targeting of the plasma membrane by gold-pHLIP is clearly seen on all images. We also observed some staining of internal organelles and nuclei membranes. Targeting of mitochondria and nuclear membranes was observed in experiments with pHLIP-coated liposomes containing lipids conjugated with fluorescent dyes and gold nanoparticles (26).

Clonogenic Assay. Clonogenic assay experiments were performed to assess cell survival after treatment of cells with gold or gold-pHLIP and radiation of treated and nontreated cells. The results of the experiments are summarized in Fig. 3 and SI Appendix, Tables S2–S5.

We tested 0, 1.5, and 3 Gray of radiation. Gold nanoparticles alone or conjugated with pHLIP were not toxic for cells in the absence of radiation. For 1.5 Gray of radiation, we observed a statistically significant 24% decrease in survival for cells treated with gold-pHLIP at low pH compared with cells treated with no gold. We also observed a statistically significant 21% decrease in survival for cells treated with gold-pHLIP at low pH compared with cells treated with gold alone. The effect of gold was not significant at 3 Gray of radiation, likely because the survival of cells at 3 Gray was low.
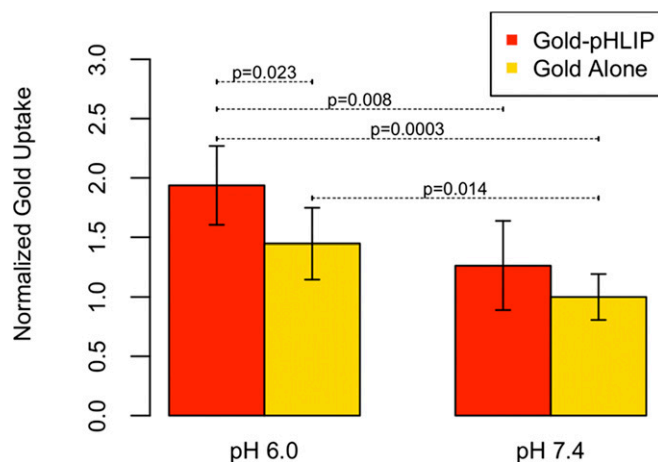

Fig. 1. Cellular uptake of gold. Values are averaged from normalized readings on a mass spectrometer, as detailed in *Methods*. All measurements are given in *SI Appendix*, Table S1. Data are normalized to gold alone at pH 7.4.

Two different methodologies were used: excess gold or gold-pHLIP was removed after treatment with cells before radiation, or excess gold and gold-pHLIP was not removed (nonremoval corresponds with the values shown in red in SI Appendix, Tables S2–S5). The clonogenic assay results in Fig. 3A include data obtained at both different methodologies. Fig. 3B shows the data obtained in the experiments when gold constructs were not removed before radiation. Surprisingly, overall, the nonremoval data have better survival than the removal data; perhaps this is a result of the removal process stressing the cells.

We assessed statistical significance for data obtained at 1.5 Gray of radiation by performing an ANOVA, summarized in Table 1 and SI Appendix, Table S6. When determining the P values between different gold treatments, we accounted for the difference in methodology as an additional variable in the analysis of variance (see *Methods* for more details). Our data clearly indicate that cell treatment with gold-pHLIP results in a statistically significant decrease in cell survival compared with a treatment with no gold (P value = 3.6×10^{-5}) or gold alone (P value = 0.015).

In a separate experiment, cells were treated with gold constructs at pH 7.4, where pHLIP is less effective at inserting into the cellular membranes. Only small and statistically insignificant differences in survival between nontreated and treated cells were seen; the data are given in SI Appendix, Tables S2, S3, and S5.

Discussion

The treatment of cancer involves a trade-off between killing all cancer cells and affecting healthy tissue and organs as little as possible. To reduce adverse effects and enhance lethal effects of radiation for cancer cells, the approaches of binary therapy were introduced. Binary radiation therapy targets cells at the biological level with a noncytotoxic agent that is "activated" by low-energy radiation, thereby destroying cancer cells wherever they may reside, while sparing normal cells in proximity to the diseased cells. A number of binary radiation therapies have been and are being explored (9, 34–36); one of the more promising approaches is based on dose enhancement through Auger electron emission secondary to the photoelectric effect dominant at low photon energies. Auger electron emission generates a cascade of low-energy electrons that travel very short distances and deposit their energy locally. The number of Auger electrons generated in targeted cells can be increased significantly by introducing material of a high atomic number (high-Z) into the target as long as the radiation energy is at or near the K, L, or M
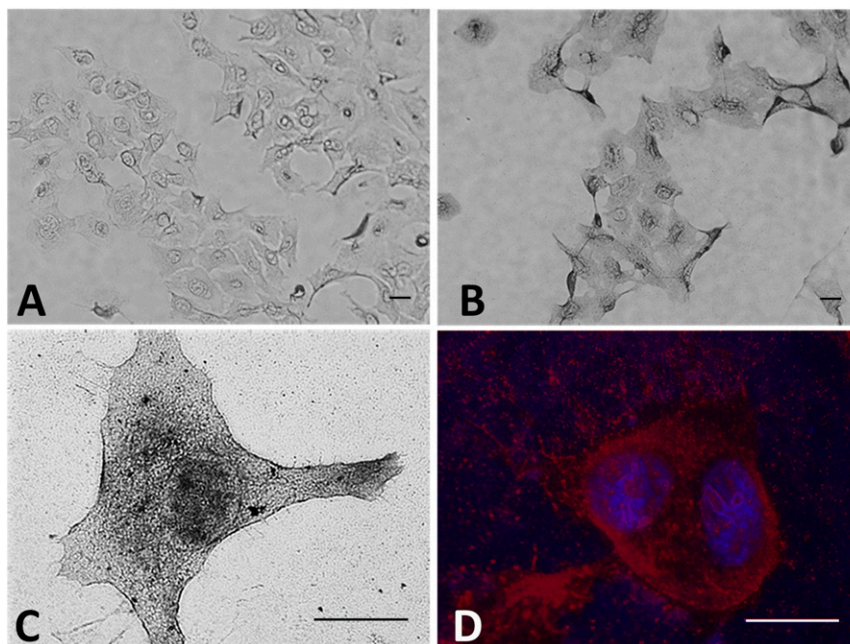
Fig. 2. Gold distribution in cells. The bright field (*A–C*) and fluorescence (*D*) images of cells treated with gold (*A*) and gold-pHLIP (*B–D*), followed by washing, fixation, and enhancement with HQ Silver, are shown at different magnifications (the bar on each image shows a 10-μm scale). The overlay of fluorescent images of nuclear stained with DAPI (blue) and cellular membrane stained with HQ Silver (red) are shown on *D*.

electron shell binding energies for the material. High-Z nanoparticles made of iodine, gadolinium, or gold are predicted to produce a clinically achievable dose enhancement of as much as 10-fold. Because low-energy electrons travel very short distances, it is crucial to deliver and accumulate high-Z material on or in cancer cells in tumors.

Our strategy is to deliver gold, which is an inert, high-Z material widely used in medicine, to cancer cells for the enhancement of radiation effects. The delivery approach we propose is based on the energy of membrane-associated folding of peptides from the pHLIP family to target cellular membranes in a pH-dependent manner (22, 24, 37). At pH < 7.0, pHLIPs insert into the lipid bilayer of the membrane, which is accompanied by a coil–helix transition and formation of a transmembrane helix. It has been shown that pHLIP delivery agents can target acidic tumors with high accuracy and deliver nanoparticles, including gold, to cancer cells in tumors (33). In this work, we show the effect of gold-pHLIP on radiation-induced cell death.

The dose enhancement depends strongly on the photon energies used for irradiation, as well as on the location and the size of gold nanoparticles. Regarding the photon energy, the ratio of gold absorption to human absorption is highest between ∼10 and 100 keV, with the ratio reaching approximately as high as 100 (2). We used 250 kVp X-rays with Sn-Thoraeus filtering to use the high relative absorption by gold while also accounting for the fact that lower-energy photons will be absorbed at too small of a depth to be useful. Regarding the location, it is very important to deliver gold nanoparticles as close as possible to cancer cells, as the dose deposited by Auger electrons increases as distance from the gold nanoparticles decreases (11). We used pHLIP to locate the gold nanoparticles to cancer cells. Regarding the nanoparticle size, it is best to use as small a gold nanoparticle size as possible to minimize the energy deposited inside the gold by Auger electrons. Simulations by McMahon et al. (11) predict an increase in relative biological effectiveness for decreasing sizes of gold nanoparticles. We used 1.4-nm-diameter gold nanoparticles.

The results of our present study indicate that pHLIP causes cells to take up more 1.4-nm gold nanoparticles than cells without pHLIP. The gold nanoparticles deposited by pHLIP mostly accumulate on the plasma membrane. As a result, gold nanoparticles delivered to cells by pHLIP can enhance radiation-induced decreases in cell survival. Gold nanoparticles tethered to the lipid bilayer of the plasma membrane by pHLIP may trigger cell death by inducing oxidation of lipids, cholesterol, and membrane proteins. The oxidized lipids are known to modify membrane physical properties, such as thickness, permeability, level of hydration and polarity, lipid transbilayer diffusion, loss of lipid asymmetry, and phase segregation, which results in apoptosis (38, 39). The exposure of phosphatidylserine lipids to the outer leaflet of the lipid bilayer, promoted by lipid oxidation, serves as a recognition signal for macrophages to phagocytose the apoptotic cell (40).

The combination of the clonogenic and uptake results suggests that pHLIP is able to enhance radiation-induced death by targeting cancer cells and increasing gold uptake. This is particularly important for future preclinical testing. Experiments on cultured cells reflect steady-state conditions, when constructs are exposed to cancer cells during the time of incubation. However, in vivo studies reflect kinetic conditions, when blood flow is high and constructs have a limited time to reach cancer cells and accumulate there. Our previous in vivo studies indicate that pHLIP targeting of 1.4-nm gold nanoparticles to tumors was 11 and 6 times higher compared with tumor targeting by gold alone (when administrated intratumorally and intravenously, respectively) (33). Thus, in an upcoming experiment on mice, we expect to observe more significant enhancement of radiation-induced cancer killing compared with data obtained on cells. This might open a new avenue for the treatment of acidic, highly metastatic tumors in humans.

Methods

Materials. Materials include nonfunctionalized nanogold (from Nanoprobes), monomaleimido nanogold (from Nanoprobes), Cys-pHLIP (synthesized and purified by CS Bio), Tris-(2-carboxyethyl) phosphine, hydrochloride (from Life Technologies), Dulbecco's modified Eagle's medium (from Sigma Aldrich), glutaraldehyde [25% (wt/wt) in water; from Sigma Aldrich], crystal violet (from Sigma Aldrich), Synaptophysin (from Molecular Probes by Life Technologies),
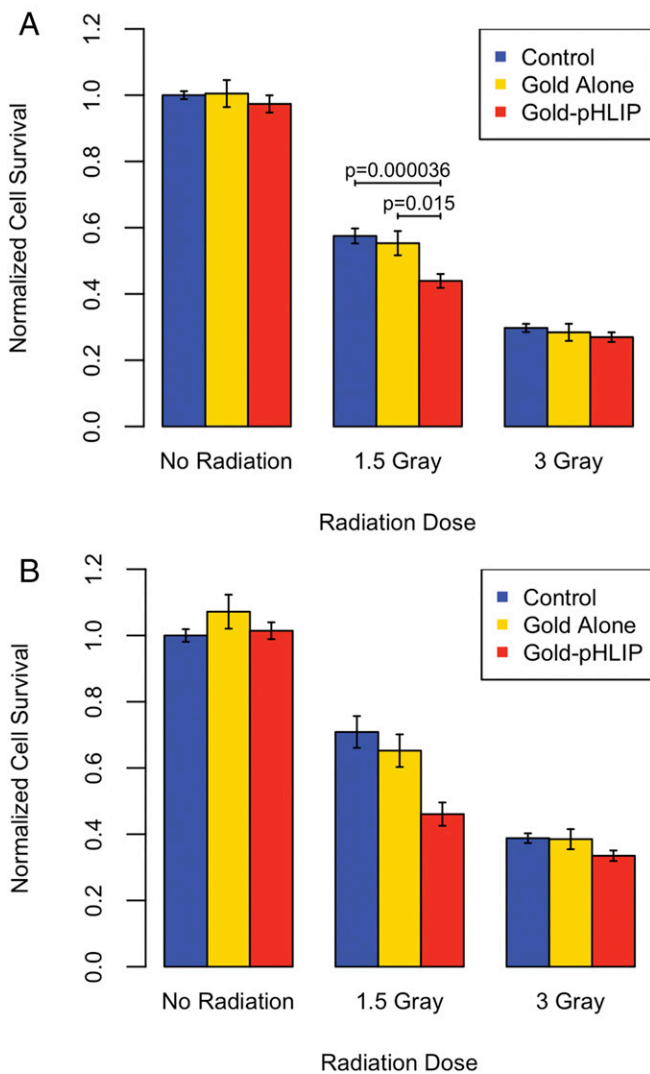
Fig. 3. Average cell survival after radiation and treatment (or no treatment, control) with gold or gold-pHLIP at pH 6.0. The data shown in *A* are from the experiments with either removal or nonremoval of excess gold before radiation. The data shown in *B* are only from the experiments with nonremoval of excess gold before radiation. Error shown is SEM.

DAPI (from Sigma Aldrich), and Silver enhancement reagent (from Nanoprobes). Cell type was human lung carcinoma A549 cells (from American Type Culture Collection).

Preparation of Gold (Gold Alone), Gold Conjugated to pHLIP (Gold-pHLIP). Gold nanoparticles were cluster gold, 1.4 nm in diameter, from Nanoprobes, Inc. Monomaleimido nanogold was conjugated to Cys-pHLIP in 40 mM phosphate buffer containing 300 mM NaCl at pH 6.5. A reducing agent, Tris-(2-carboxyethyl) phosphine, was added into the reaction mixture (10× excess compared with pHLIP) to reduce pHLIP-S-S-pHLIP dimers and promote reaction with gold-maleimide. The reaction vial was incubated overnight at room temperature on shaker. The next day, the gold-pHLIP conjugates were purified using Amicon Ultra (10 K) centrifugal filters according to company-recommended protocol. The product was then lyophilized and redissolved in DMSO. The concentration of peptide and nanogold was determined by absorbance at 280 nm ($\varepsilon = 13{,}940$ M$^{-1}\cdot$cm^{-1}) and 420 nm ($\varepsilon = 155{,}000$ M$^{-1}\cdot$cm^{-1}), respectively. Nonfunctionalized gold (gold alone) was dissolved in DMSO and quantified using absorbance of gold at 420 nm.

Cellular Uptake of Gold. Approximately 1 million cells A549 were treated with 0.3 μM of either gold alone or gold-pHLIP in cell suspension in serum-free DMEM at pH 6.0 and 7.4 for 1 h. One nanogold particle (1.4 nm in diameter) contains, on average, 60 gold atoms, and 0.3 μM particles in 0.5 mL solution correspond to 1.8 μg of gold. After 1 h of treatment, the cells were pelleted using centrifugation (2,000 rpm × *g* for 5 min), followed by removal of treatment and washing cells with PBS three times. The cells were then dissolved in concentrated nitric acid, followed by sonication for about 2 h. Concentrated solution samples were diluted to give 2% (wt/vol) nitric acid and analyzed via inductively coupled plasma mass spectroscopy (Thermo-Scientific ×7 series) against calibration standards (IMS 103; UltraScientific).

Cellular Distribution of Gold. About 20,000 A549 cells were seeded on collagen-coated glass-bottom dishes (MatTek) in 200 μL volume. The next day, cells were treated for 1 h with gold and gold-pHLIP at 0.5 μM concentration at pH 6.0 in DMEM with no FBS. After treatment, the cells were washed 3 times with PBS, followed by fixation in 4% (wt/vol) formaldehyde for 20 min. The cells were permeabilized with 0.3% Triton ×100 for 5 min, followed by washing with PBS and deionized water. Next, the cells were developed with freshly prepared HQ Silver reagent (Nanoprobes) for about 20 min, followed by washing with deionized water. Finally, the cells were stained with 5 μM DAPI in PBS for 5 min, followed by washing with deionized water. The cells were imaged using light microscope in a bright field regime to visualize gold enhanced by silver, and in the fluorescent regime to monitor DAPI and silver fluorescence, using cut-off filters (ex:em 360 nm/460 nm and ex:em 542 nm/620 nm, respectively).

Irradiation of Cells. Irradiation was performed using a Philips RT 250 X-ray machine at settings of 250 kVp and 15 mA. A 0.4-mm Sn-Thoraeus Filter was used. The half-value thickness for this setup is listed as 2.8 mm Cu. The dose rate was ~1.5 Gray/minute for each irradiation. Calibration readings were performed before each measurement, using a Radcal 2026C dosimeter, and the reading was corrected for differences in temperature and pressure from standard temperature and pressure. The irradiation dose varied by ~7% between the center of the cell dish and the rightmost well in the irradiation plate that we used (there was ~1–2% variation in the leftmost well); the rightmost well was only used in experiments 7–11, and there were always at least three wells used per treatment.

Clonogenic Assay. The day before irradiation, 25,000 A549 cells per well were seeded in 48-well plates. One plate with different treatment conditions was used for each radiation dose. The next day, the cells were treated with no gold, gold alone, or gold-pHLIP at 8 μM concentration in 300 μL DMEM with no FBS at pH 6.0 for 3 h. In experiment 11, the medium pH during treatment was 7.4 instead of 6.0. In one set of experiments, the excess gold was removed and 500 μL fresh DMEM at pH 7.4 with 10% FBS was added. In the other set of experiments, the excess gold was not removed, and then 200 μL fresh DMEM at pH 7.4 with 25% serum was added into wells to have 10% of FBS in a final volume in the well. The treatment period was ~3 h.

Cells were irradiated as described in the irradiation methods; control cells accompanied the irradiated cells to and from the X-ray machine. Irradiated cells were dissociated and combined for each treatment type, counted (using a Coulter Counter Z1 instrument from Beckman Coulter for experiments 1–11 and an Auto T4 instrument from Nexcelom Bioscience for experiments 12–17), and then reseeded in a six-well plate. Two hundred cells per well were seeded for 0- and 1.5-Gray radiation doses, and 500 cells per well were seeded for 3-Gray radiation dose. In general, six wells were seeded per treatment type; the number of entries in *SI Appendix*, Table S2 is the number of wells. A table entry with 12 values represents a treatment that was done twice in the same experiment, with the results combined. After ~10 d, each well was fixed and stained using a 2-mL mixture of 4% glutaraldehyde and 0.5% crystal violet in distilled water. Stained cell colonies were hand-counted under a microscope. A colony was defined as a distinct group of cells that contained 50 or more cells.

Table 1. Summary of ANOVA results for 1.5 Gray radiation

Model [normalized survival = treatment + removal + (treatment · removal)]	P values
No gold vs. gold-pHLIP	3.64×10^{-5}
Gold-pHLIP vs. gold alone	0.015
No gold vs. gold alone	0.832
Removal vs. nonremoval	5.95×10^{-6}

Detailed results are in *SI Appendix*, Table S6.

Analysis of Cellular Uptake Data. The values in *SI Appendix*, Table S1 are six readings from a mass spectrometer. *P* values for statistical significance were computed using the *t* test, because the between-reading variance was much greater than the error in each reading.

Analysis of Clonogenic Assay Data. To calculate statistical significance, the data summarized in *SI Appendix*, Tables S2–S5 were analyzed using an ANOVA, followed by a post hoc test using Tukey's Honest Significant Difference. Each individual measurement from the clonogenic assay dish was treated as a biological replicate and normalized to the average of the "0 Radiation, No Gold" measurements from the same experiment.

The linear model fitted for the ANOVA had three variables: normalized survival (dependent variable), gold treatment (independent variable), and removal/nonremoval of excess gold (independent variable). We left the data for 0 radiation out of the analysis because normalizing by the "0 Radiation, No Gold" data points introduces a correlation if we use the data by which we are normalizing. We analyzed the data for 1.5 Gray and 3 Gray separately because we were only really interested in the effect at 1.5 Gray.

In the 1.5-Gray data, the interaction term between gold treatment and removal/nonremoval was significant. This is consistent with the gold treatments having different effectiveness depending on whether or not the excess gold was removed.

We also did one experiment at high pH, as mentioned in the *Results*. This was analyzed with a separate analysis of variance. The data are included as experiment 11 in *SI Appendix*, Tables S2, S3, and S5.

In Fig. 3, error shown is the SEM (41). SE was calculated using R, as SD divided by square root of the number of samples. In checking the procedure for this calculation, we used StatPlus, version v5 (AnalystSoft Inc.).

1. Black KC, et al. (2008) Gold nanorods targeted to delta opioid receptor: Plasmon-resonant contrast and photothermal agents. *Mol Imaging* 7(1):50–57.
2. Hainfeld JF, Dilmanian FA, Slatkin DN, Smilowitz HM (2008) Radiotherapy enhancement with gold nanoparticles. *J Pharm Pharmacol* 60(8):977–985.
3. Hainfeld JF, Slatkin DN, Focella TM, Smilowitz HM (2006) Gold nanoparticles: A new X-ray contrast agent. *Br J Radiol* 79(939):248–253.
4. Huang X, Jain PK, El-Sayed IH, El-Sayed MA (2007) Gold nanoparticles: Interesting optical properties and recent applications in cancer diagnostics and therapy. *Nanomedicine (Lond)* 2(5):681–693.
5. Jain PK, El-Sayed MA (2007) Universal scaling of plasmon coupling in metal nanostructures: Extension from particle pairs to nanoshells. *Nano Lett* 7(9):2854–2858.
6. Mahmoud MA, El-Sayed MA (2010) Gold nanoframes: Very high surface plasmon fields and excellent near-infrared sensors. *J Am Chem Soc* 132(36):12704–12710.
7. von Maltzahn G, et al. (2009) Computationally guided photothermal tumor therapy using long-circulating gold nanorod antennas. *Cancer Res* 69(9):3892–3900.
8. Babaei M, Ganjalikhani M (2014) The potential effectiveness of nanoparticles as radio sensitizers for radiotherapy. *Bioimpacts* 4(1):15–20.
9. Hainfeld JF, Slatkin DN, Smilowitz HM (2004) The use of gold nanoparticles to enhance radiotherapy in mice. *Phys Med Biol* 49(18):N309–N315.
10. Jain S, et al. (2011) Cell-specific radiosensitization by gold nanoparticles at megavoltage radiation energies. *Int J Radiat Oncol Biol Phys* 79(2):531–539.
11. McMahon SJ, et al. (2011) Biological consequences of nanoscale energy deposition near irradiated heavy atom nanoparticles. *Sci Rep* 2011;1:18.
12. Sonvico F, et al. (2005) Folate-conjugated iron oxide nanoparticles for solid tumor targeting as potential specific magnetic hyperthermia mediators: Synthesis, physicochemical characterization, and in vitro experiments. *Bioconjug Chem* 16(5):1181–1188.
13. Kirpotin DB, et al. (2006) Antibody targeting of long-circulating lipidic nanoparticles does not increase tumor localization but does increase internalization in animal models. *Cancer Res* 66(13):6732–6740.
14. Huang X, et al. (2010) A reexamination of active and passive tumor targeting by using rod-shaped gold nanocrystals and covalently conjugated peptide ligands. *ACS Nano* 4(10):5887–5896.
15. Hainfeld JF, et al. (2011) Micro-CT enables microlocalisation and quantification of Her2-targeted gold nanoparticles within tumour regions. *Br J Radiol* 84(1002):526–533.
16. Herold DM, Das IJ, Stobbe CC, Iyer RV, Chapman JD (2000) Gold microspheres: A selective technique for producing biologically effective dose enhancement. *Int J Radiat Biol* 76(10):1357–1364.
17. Damaghi M, Wojtkowiak JW, Gillies RJ (2013) pH sensing and regulation in cancer. *Front Physiol* 4:370.
18. Gillies RJ, Verduzco D, Gatenby RA (2012) Evolutionary dynamics of carcinogenesis and why targeted therapy does not work. *Nat Rev Cancer* 12(7):487–493.
19. Robey IF, et al. (2009) Bicarbonate increases tumor pH and inhibits spontaneous metastases. *Cancer Res* 69(6):2260–2268.
20. Adochite RC, et al. (2014) Targeting breast tumors with pH (low) insertion peptides. *Mol Pharm* 11(8):2896–2905.
21. Cruz-Monserrate Z, et al. (2014) Targeting pancreatic ductal adenocarcinoma acidic microenvironment. *Sci Rep* 4:4410.
22. Andreev OA, Engelman DM, Reshetnyak YK (2014) Targeting diseased tissues by pHLIP insertion at low cell surface pH. *Front Physiol* 5:97.
23. Viola-Villegas NT, et al. (2014) Understanding the pharmacological properties of a metabolic PET tracer in prostate cancer. *Proc Natl Acad Sci USA* 111(20):7254–7259.
24. Weerakkody D, et al. (2013) Family of pH (low) insertion peptides for tumor targeting. *Proc Natl Acad Sci USA* 110(15):5834–5839.
25. An M, Wijesinghe D, Andreev OA, Reshetnyak YK, Engelman DM (2010) pH-(low)-insertion-peptide (pHLIP) translocation of membrane impermeable phalloidin toxin inhibits cancer cell proliferation. *Proc Natl Acad Sci USA* 107(47):20246–20250.
26. Yao L, Daniels J, Wijesinghe D, Andreev OA, Reshetnyak YK (2013) pHLIP®-mediated delivery of PEGylated liposomes to cancer cells. *J Control Release* 167(3):228–237.
27. Wijesinghe D, Arachchige MC, Lu A, Reshetnyak YK, Andreev OA (2013) pH dependent transfer of nano-pores into membrane of cancer cells to induce apoptosis. *Sci Rep* 3:3560.
28. Emmetiere F, et al. (2013) (18)F-labeled-bioorthogonal liposomes for in vivo targeting. *Bioconjug Chem* 24(11):1784–1789.
29. Sosunov EA, et al. (2013) pH (low) insertion peptide (pHLIP) targets ischemic myocardium. *Proc Natl Acad Sci USA* 110(1):82–86.
30. Han L, Ma H, Guo Y, Kuang Y, He X, Jiang C (2013) pH-controlled delivery of nanoparticles into tumor cells. *Adv Healthc Mater* 2(11):1435–1439.
31. Zhao Z, et al. (2013) A controlled-release nanocarrier with extracellular pH value driven tumor targeting and translocation for drug delivery. *Angew Chem Int Ed Engl* 52(29):7487–7491.
32. Davies A, Lewis DJ, Watson SP, Thomas SG, Pikramenou Z (2012) pH-controlled delivery of luminescent europium coated nanoparticles into platelets. *Proc Natl Acad Sci USA* 109(6):1862–1867.
33. Yao L, et al. (2013) pHLIP peptide targets nanogold particles to tumors. *Proc Natl Acad Sci USA* 110(2):465–470.
34. Morris KN, Weil MD, Malzbender R (2006) Radiochromic film dosimetry of contrast-enhanced radiotherapy (CERT). *Phys Med Biol* 51(22):5915–5925.
35. Norman A, et al. (1997) X-ray phototherapy for canine brain masses. *Radiat Oncol Investig* 5(1):8–14.
36. Tisljar-Lentulis G, Feinendegen LE, Bond VP (1973) [Biological radiation effects of inclusion of moderately heavy nuclei into the tissue and use of soft roentgen rays]. *Strahlentherapie* 145(6):656–662.
37. Karabadzhak AG, et al. (2012) Modulation of the pHLIP transmembrane helix insertion pathway. *Biophys J* 102(8):1846–1855.
38. Kinnunen PK, Kaarniranta K, Mahalka AK (2012) Protein-oxidized phospholipid interactions in cellular signaling for cell death: From biophysics to clinical correlations. *Biochim Biophys Acta* 1818(10):2446–2455.
39. Volinsky R, Kinnunen PK (2013) Oxidized phosphatidylcholines in membrane-level cellular signaling: From biophysics to physiology and molecular pathology. *FEBS J* 280(12):2806–2816.
40. Leventis PA, Grinstein S (2010) The distribution and function of phosphatidylserine in cellular membranes. *Annu Rev Biophys* 39:407–427.
41. Altman DG, Bland JM (2005) Standard deviations and standard errors. *BMJ* 331(7521):903.